Sedimentation of particles

Élisabeth Guazzelli

Université de Paris, CNRS, Matière et Systèmes Complexes (MSC)

from Chapter 6 of *A Physical Introduction to Suspension Dynamics* CUP 2012
by É. Guazzelli & J. F. Morris (illustrations by S. Pic)

and *Fluctuations and instability in sedimentation* Annual Review of Fluid Mechanics 2011

by É. Guazzelli & J. E. Hinch

Collective behavior of particles in fluids
IHP Paris, December 14-17, 2020

Part I: Falling clouds

1. 1, 2, 3 . . . spheres
2. A cloud of spheres
   - Stability of the cloud
   - Influence of initial shape on subsequent evolution
   - Leakage and breakup
3. And also a cloud of fibers
4. Beyond Stokes: A cloud at finite Reynolds number
   - Spheres at finite inertia
   - The regimes of evolution for a falling cloud
   - Instability and breakup
5. And beyond . . .

Part II: Settling particles

Part I

Falling clouds

Dispersion of Sphagnum Moss Spores
Whitaker & Edwards Science 2010

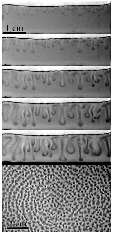

Bioconvection
Jánosi, Kessler & Horváth PRE 1998

J. Fluid Mech. (1997), *vol.* 340, *pp.* 161–175. Printed in the United Kingdom 161

Break-up of a falling drop containing dispersed particles

By J. M. NITSCHE[1] AND G. K. BATCHELOR[2]

[1]Department of Chemical Engineering, State University of New York at Buffalo, Buffalo, NY 14260, USA

[2]Department of Applied Mathematics and Theoretical Physics, University of Cambridge, Silver Street, Cambridge CB3 9EW, UK

(Received 25 August 1996 and in revised form 22 January 1997)

We shall present a numerical investigation of hydrodynamic dispersion in a system containing an interface which separates a random dispersion of prescribed particle concentration on one side from clear fluid on the other side. Specifically, we consider the motion under gravity of particles within a blob (a convenient term for a finite volume of a dispersion of particles in liquid) comprising a large number N of particles initially distributed randomly in liquid with uniform mean concentration within a prescribed closed surface, and inquire as to its subsequent time evolution. The particles will tend to spread out from each other, and questions of interest are therefore: do particles leave the blob, and if so how, and what is the lifetime of the blob as a cohesive entity? A spherical blob shape is especially well suited to a study of random particle migration across interfaces because the gravity-driven flow system maintains essentially constant form. Thus, the migration process can be observed without the complication of significant deformation of the blob as a whole. As noted above, it is not possible to specify the flux of particles across such an interface in terms of a particle diffusivity of the conventional kind. Some alternative analytical description of the dispersion process at the interface is required.

1. 1, 2, 3 . . . spheres
2. A cloud of spheres
   - Stability of the cloud
   - Influence of initial shape on subsequent evolution
   - Leakage and breakup
3. And also a cloud of fibers
4. Beyond Stokes: A cloud at finite Reynolds number
   - Spheres at finite inertia
   - The regimes of evolution for a falling cloud
   - Instability and breakup
5. And beyond . . .

Sedimentation of a single sphere for $Re_p = aU_S/\nu \ll 1$

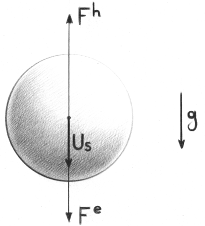

Force balance: $\mathbf{F^e} + \mathbf{F^h} = 0$

$$\frac{4}{3}\pi a^3(\rho_p - \rho)\mathbf{g} - 6\pi\mu a\mathbf{U} = 0$$

Stokes velocity

$$\mathbf{U_S} = 2(\rho_p - \rho_f)a^2\mathbf{g}/9\mu$$

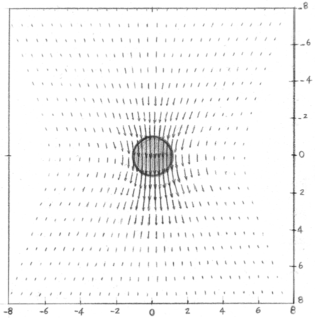

Slow-decay disturbance $\sim O(\frac{aU_S}{r})$

Stokes 1851

Sedimentation of a pair of identical spheres

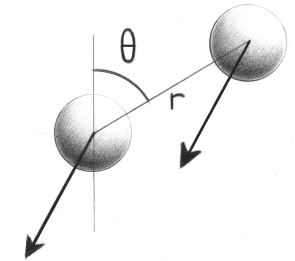

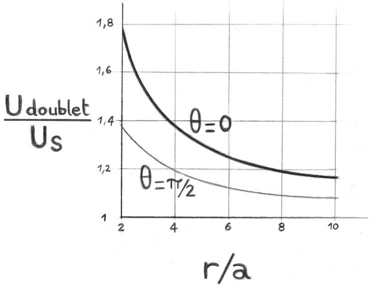

$$\frac{U_{\mathrm{doublet}}}{U_S} = 1 + \frac{3a}{2r} \quad \text{for} \quad \theta = 0,$$
$$\frac{U_{\mathrm{doublet}}}{U_S} = 1 + \frac{3a}{4r} \quad \text{for} \quad \theta = \frac{\pi}{2}$$

Two identical spheres fall at the same velocity and therefore do not change their orientation and separation

Method of reflection: Smoluchowski Bull. Acad. Sci. Cracovie 1911

Sedimentation of a triplet

The three-body problem!

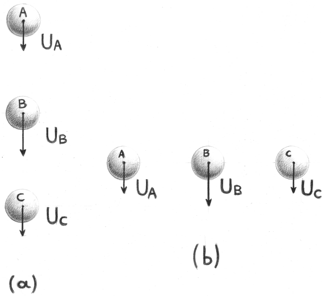

The particles do not maintain constant separation: the middle particle B falls faster

- case (a):

$$\frac{U_A}{U_S} = \frac{U_C}{U_S} = 1 + \frac{3}{2}\left(\frac{a}{r} + \frac{a}{2r}\right) = 1 + \frac{9a}{4r}$$
$$\frac{U_B}{U_S} = 1 + \frac{3}{2}\left(\frac{a}{r} + \frac{a}{r}\right) = 1 + \frac{3a}{r}$$

- case (b):

$$\frac{U_A}{U_S} = \frac{U_C}{U_S} = 1 + \frac{3}{4}\left(\frac{a}{r} + \frac{a}{2r}\right) = 1 + \frac{9a}{8r}$$
$$\frac{U_B}{U_S} = 1 + \frac{3}{4}\left(\frac{a}{r} + \frac{a}{r}\right) = 1 + \frac{3a}{2r}$$

Stokeslet simulation of a triplet

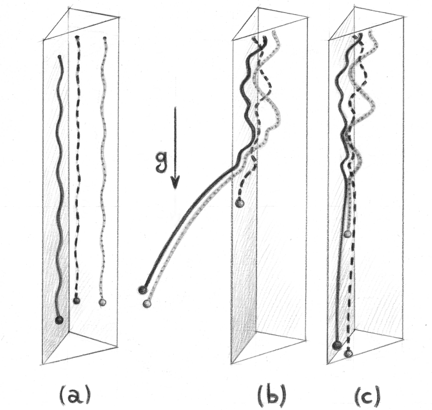

- case (a): particles positioned at the vertices of an horizontal isosceles triangle
- case (b): random initial configuration
- case (c): random initial configuration differing from (b) by only an $O(10^{-3})$ perturbation in the horizontal coordinates of one particle

Sensitivity to initial configurations: signature of **chaotic behavior** originating in the long-range and many-body character of the hydrodynamic interactions

Spherical cloud of N spheres

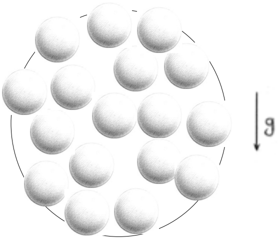

Balance between gravitational and drag forces

$$N\frac{4}{3}\pi a^3(\rho_p - \rho)\mathbf{g} - 2\pi\mu\frac{2+3\frac{\mu_s}{\mu}}{\frac{\mu_s}{\mu}+1}R\,\mathbf{V} = 0$$

- Drag force of a drop

$$\mathbf{F^h} = -2\pi\mu\frac{2+3\frac{\mu_s}{\mu}}{\frac{\mu_s}{\mu}+1}R\,\mathbf{V}$$

Hadamard C. R. Acad. Sci. Paris 1911

Rybczyński Bull. Acad. Sci. Cracovie 1911

- Settling velocity

$$\mathbf{V} = \frac{N\frac{4}{3}\pi a^3(\rho_p - \rho)\mathbf{g}}{2\pi\mu\frac{2+3\frac{\mu_s}{\mu}}{\frac{\mu_s}{\mu}+1}R} \approx \frac{N\frac{4}{3}\pi a^3(\rho_p - \rho)\mathbf{g}}{5\pi\mu R}$$

Continuous spherical distribution of excess mass

Flow field inside a falling drop

in the drop reference frame

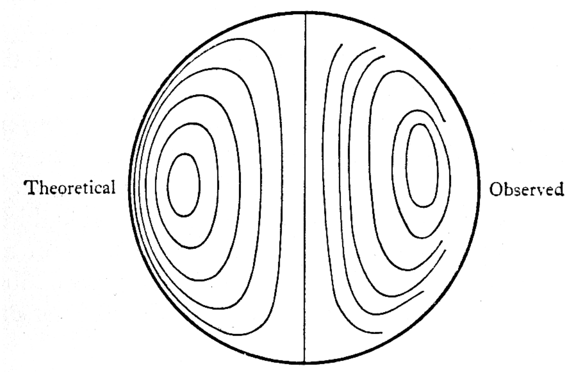

from Batchelor *An Introduction to Fluid Dynamics* CUP 1967
after Spells Proc. Phys. Soc. 1952

Toroidal circulation

Stability of the cloud?

- "A spherical blob shape is especially well suited to a study of random particle migration across interface because the gravity-driven flow **maintains essentially constant form**"

  Nitsche & Batchelor JFM 1997

- "An initially spherical blob **does not substantially change its shape** when falling"

  Machu, Meile, Nitsche & Schaflinger JFM 2000

- "In the case of low Reynolds numbers, the suspension drop **retains a roughly spherical shape** while settling"

  Bosse, Kleiser, Härtel & Meiburg PoF 2005

But the cloud is unstable!

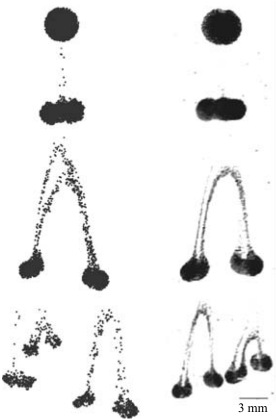

Metzger, Nicolas & Guazzelli JFM 2007

Point-force model: The Stokeslet

- Minimal description: **only far-field and strictly** $Re = 0$

$$\dot{\mathbf{r}}_i = \mathbf{U_S} + \frac{\mathbf{F^e}}{8\pi\mu} \cdot \sum_{j\neq i} \left(\frac{\mathbf{I}}{|\mathbf{r^*_{ij}}|} + \frac{\mathbf{r_{ij}r_{ij}}}{|\mathbf{r^*_{ij}}|^3} \right)$$

with $\mathbf{r}_{ij} \equiv \mathbf{r}_i - \mathbf{r}_j$

- Dimensionless equations (length-scale $= R_0$ and velocity-scale $= V_0 = \frac{N_0 F}{5\pi\mu R_0}$ of the initially spherical cloud)

$$\dot{\mathbf{r}^*}_i = \frac{5R_0}{6N_0 a} \cdot \mathbf{e}_g + \frac{5}{8N_0} \sum_{j\neq i} \left(\frac{\mathbf{I}}{|\mathbf{r^*_{ij}}|} + \frac{\mathbf{r_{ij}r_{ij}}}{|\mathbf{r^*_{ij}}|^3} \right) \cdot \mathbf{e_g}$$

Ekiel-Jeżewska, Metzger & Guazzelli PoF 2006
Metzger, Nicolas & Guazzelli JFM 2007

Evolution of the cloud

Break-up probability and time

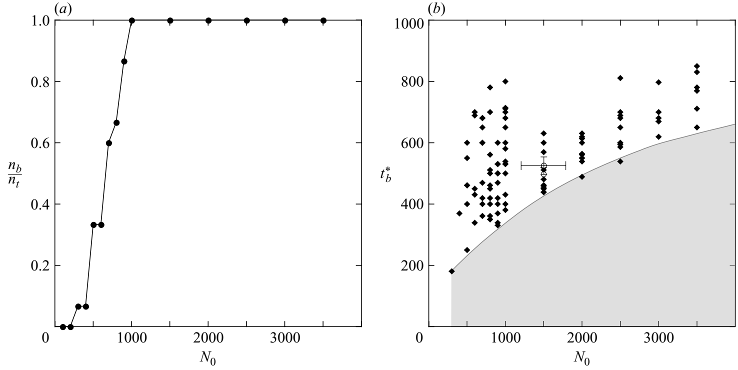

Sole dependance on N_0

Successive numerical-cloud profiles

Positions of the point particles integrated over the azimuthal angle

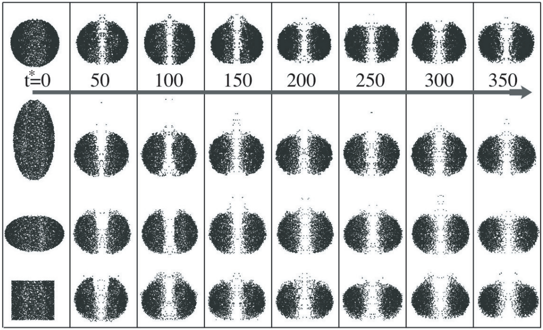

At long times, the cloud always reduces to a torus

Successive experimental-cloud profiles

Photographs of the clouds: (a) nearly spherical and (b) prolate initial shapes

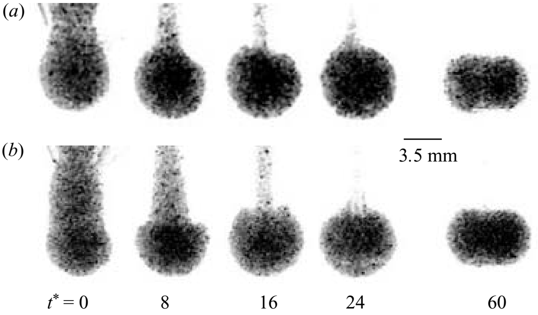

At long times, a torus is also recovered in the experiments

Evolution of the horizontal-to-vertical aspect ratio γ

Different initial shapes: (a) numerical simulations and (b) experiments

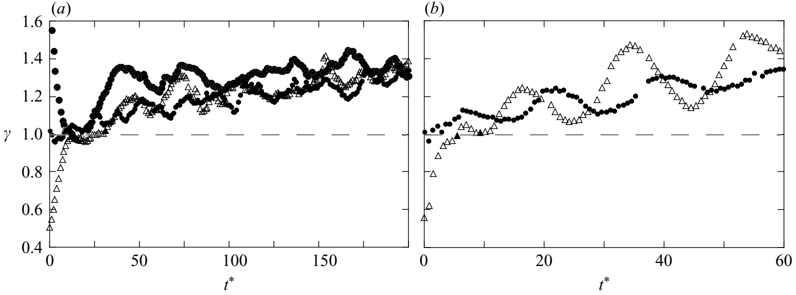

Larger horizontal expansion of the cloud in the experiments
Excluded volume effects not accounted for in the model!

Mechanism leading to particle leakage from the cloud

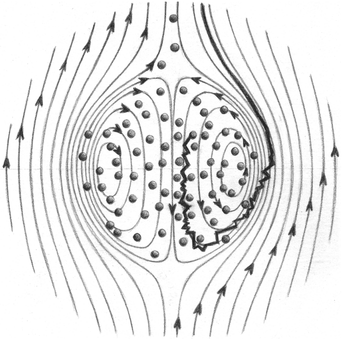

Departure from the closed toroidal circulation due to local unsteadiness of the velocity of the particles

Instability and breakup

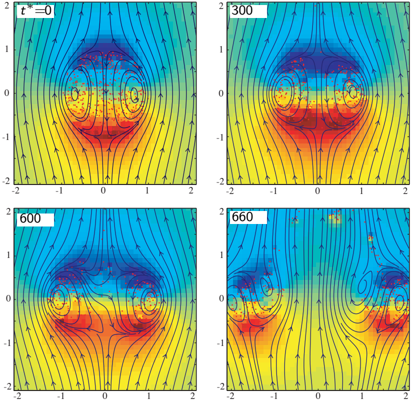

Flow and pressure fields computed at successive times in the vertical plane through the vertical axis of symmetry and in the instantaneous reference frame of the cloud

Physical insight using a cloud having a torus shape

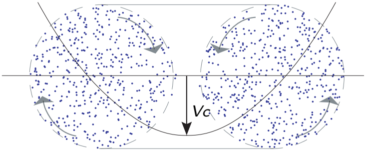

in the cloud reference frame

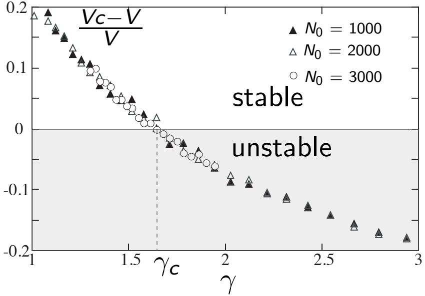

- For $\gamma \geqslant \gamma_c = 1.64 \pm 0.05$, the streamlines pass through the hole in the centre of the torus
- **Break-up = change in flow configuration created by the point particles** when γ reaches γ_c

Criterion for destabilization

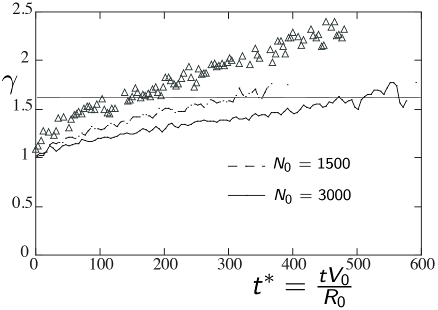

- In point-particle simulations for different $N_0 = 1500$ and 3000, break-up at $\gamma_c \approx 1.64$
- In experiments for $N_0 \approx 1500$ ($\phi = 20 \pm 3\%$), break-up occurs for a larger $\gamma_c \approx 2.4$

Sedimentation of a single fiber

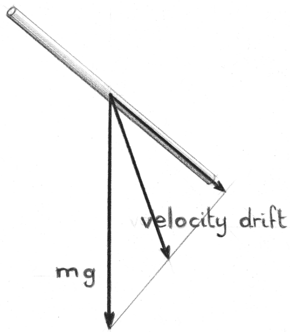

- Drag for perpendicular motion approximately twice that for parallel motion
- A fiber parallel to gravity settles approximately twice as fast as a fiber perpendicular to gravity
- A fiber inclined at an angle to vertical does not settle vertically but drifts sideways

Coupling between orientation and velocity

Batchelor JFM 1970; Cox JFM 1970

Faster evolution of the cloud of fibers!

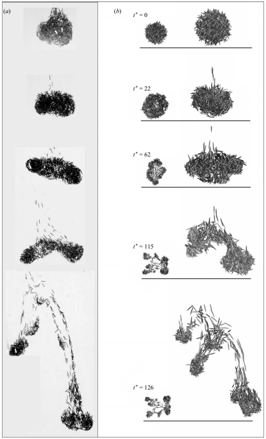

Minimal description: The “fiblet” (point-fiber)

- Dimensionless equation for translational velocity

$$\dot{\mathbf{r}}^*_\alpha = \frac{5c}{8N_0}\left(\mathbf{I} + \mathbf{p}_\alpha \mathbf{p}_\alpha\right)\cdot \mathbf{e}_g + \frac{5}{8N_0}\sum_{\beta\neq\alpha}^{N_0}\left(\frac{\mathbf{I}}{|\mathbf{r}^*|} + \frac{\mathbf{r}^*\mathbf{r}^*}{|\mathbf{r}^*|^3}\right)\cdot \mathbf{e}_g$$

with $c = 2R_0 \ln(2A)/l$ and aspect ratio $A = l/d$

- Dimensionless equation for rotational velocity

$$\dot{\mathbf{p}}^*_\alpha = \frac{5}{8N_0}\left(\mathbf{I} - \mathbf{p}_\alpha \mathbf{p}_\alpha\right)\cdot \sum_{\beta\neq\alpha}^{N_0}\left[\frac{(\mathbf{r}^*\cdot\mathbf{p}_\alpha)\,\mathbf{I} - \mathbf{p}_\alpha\mathbf{r}^* - \mathbf{r}^*\mathbf{p}_\alpha}{|\mathbf{r}^*|^3} + \frac{3\,(\mathbf{r}^*\cdot\mathbf{p}_\alpha)\,\mathbf{r}^*\mathbf{r}^*}{|\mathbf{r}^*|^5}\right]\cdot \mathbf{e}_g$$

Self-term prevails over hydrodynamic interactions between the particles as c becomes large relative to N_0

Park, Metzger, Guazzelli & Butler JFM 2010

Evolution of the fiblet cloud

Break-up time

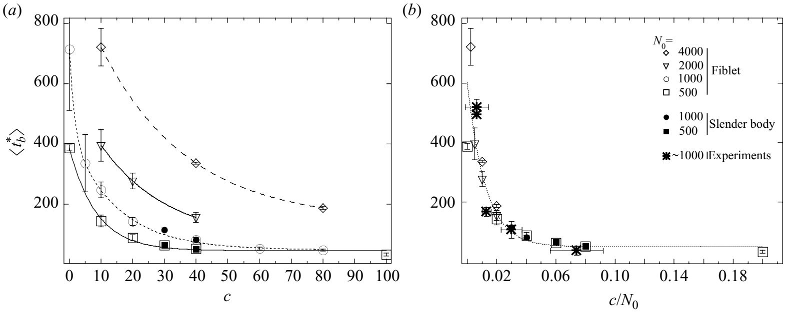

Sole dependance on c/N_0 (self motion of the anisotropic particles)

Particle anisotropy accelerates the expansion of the cloud and leads to a faster break-up

1. 1, 2, 3 . . . spheres
2. A cloud of spheres
   - Stability of the cloud
   - Influence of initial shape on subsequent evolution
   - Leakage and breakup
3. And also a cloud of fibers
4. Beyond Stokes: A cloud at finite Reynolds number
   - Spheres at finite inertia
   - The regimes of evolution for a falling cloud
   - Instability and breakup
5. And beyond . . .

Limit of Stokes approximation

Influence of inertia far from the sphere

Far from the fixed sphere: $\mathbf{U} + \mathbf{u}$ with $\mathbf{u} = O(Ua/r)$ leading Stokeslet

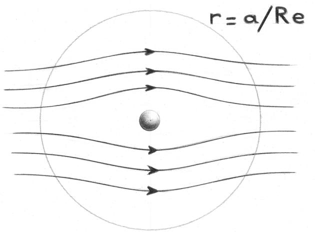

Ratio between inertial and viscous effects:

$$\frac{|\rho\left[(\mathbf{U}+\mathbf{u})\cdot\nabla\right](\mathbf{U}+\mathbf{u})|}{|\mu\nabla^2(\mathbf{U}+\mathbf{u})|} \sim \frac{U^2 a}{r^2} \Big/ \frac{\nu U a}{r^3} \sim \frac{Ua}{\nu}\frac{r}{a} \left(= Re_p \frac{r}{a}\right)$$

$$\sim O(1) \quad \text{for} \quad r/a = O(Re_p^{-1})$$

Oseen solution for a translating sphere

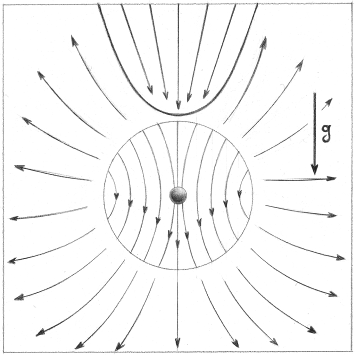

- Near field: Stokes solution
- Far field:
  - Radial outflow
    $\sim 1/r^2$
    compensated by
  - Wake inflow
    $\sim 1/r$

Loss of fore-aft symmetry above inertial screening length $\ell = a/Re_p = \nu/U_0$

Oseen Ark. Mat. Astron. Fys. 1910

2 settling spheres at finite inertia

Drafting, kissing, and tumbling

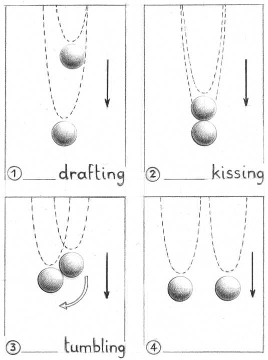

Interaction more complex due to the nature of the fluid velocity due to a sphere (wake behind the sphere and radial source flow in other directions)

Fortes, Joseph & Lundgren JFM 1987
Feng, Hu, & Joseph JFM 1994

Dimensional analysis for a sedimenting cloud at finite *Re*

- Seven independent physical quantities:
  - Viscosity μ and density ρ_f of the fluid
  - Radius a and density ρ_p of the particles
  - Radius R_0 and number of particles N_0 of the cloud
  - Gravitational acceleration g
- Underlying consideration: long range interactions dominant – short range interactions neglected (no dependance on a/R_0)
- Appropriate dimensionless numbers:
  - N_0 or $\phi = N_0(a/R_0)^3$
  - Dimensionless inertial length $\ell^* = \ell/R_0 = (a/R_0)/Re_p$ or particle Reynolds number $Re_p = U_0 a\rho_f/\mu = (a/R_0)/\ell^*$
  - Cloud Reynolds number $Re_c = V_0 R_0 \rho_f/\mu$
  - Stokes number $St = \frac{2}{9}(\rho_p/\rho_f)Re_p \ll 1$

Regimes of evolution for a sedimenting cloud

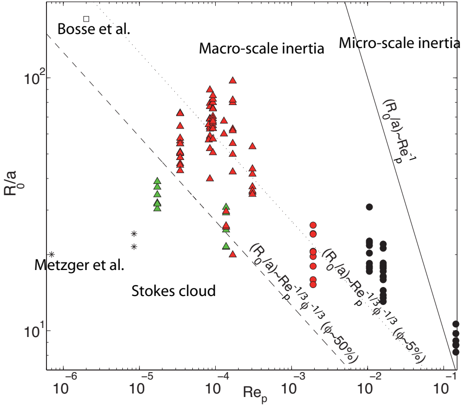

- Stokes cloud: Re_p and $Re_c \ll 1$
- Macro-scale inertia: $Re_c(\sim \phi Re_p R_0^3/a^3) \sim 1$
- Micro-scale inertia: $\ell = a/Re_p \sim R_0$

Subramanian & Koch JFM 2008

Pignatel, Nicolas & Guazzelli JFM 2011

Macro-scale inertia

Navier-Stokes equations solved in Fourier space – Lagrangian point-particle tracking – two-way coupling + Experiments in 'Macro-scale inertia' regime

Bosse, Kleiser, Härtel & Meiburg PoF 2005; Pignatel, Nicolas & Guazzelli JFM 2011

Micro-scale inertia

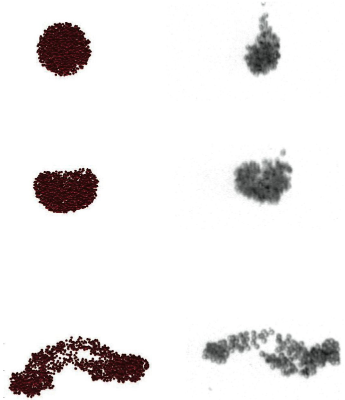

Oseenlet simulations + Experiments in 'Micro-scale inertia' regime
Pignatel, Nicolas & Guazzelli JFM 2011

Oseenlet simulations

- Steady Oseen equations still linear (but no longer reversible)

$$\dot{r}_i^\alpha = U_0\delta_{i3} + \frac{F}{8\pi\mu}\sum_{\alpha\neq\beta}\left\{\frac{r_i}{r^2}\left[\frac{2\ell}{r}(1-E)-E\right]+\frac{E}{r}\delta_{i3}\right\}$$

with $r_i \equiv r_i^\alpha - r_i^\beta$, $E = \exp(-(1+x_3/r)r/2\ell)$, gravity $i=3$

- Dimensionless equations (length-scale $= R_0$ and velocity-scale $= V_0 = \frac{N_0 F}{5\pi\mu R_0}$ of the initially spherical cloud)

$$\dot{r^*}_i^\alpha = \frac{5}{8N_0}\sum_{\alpha\neq\beta}\left\{\frac{r_i^*}{r^{*2}}\left[\frac{2\ell^*}{r^*}(1-E)-E\right]+\frac{E}{r^*}\delta_{i3}\right\}$$

Pignatel, Nicolas & Guazzelli JFM 2011

Micro-scale inertia: Simulations

Oseenlet simulations with $N_0 = 2000$ and $\ell^* = 1$

Mechanisms for torus transition and breakup

$N_0 = 2000$ and $\ell^* = 1$ (left) and $\ell^* = 20$ (right)

- Evolution toward a torus shape due to fluid inflow instead of particle depletion in Stokes regime
- Breakup at larger aspect ratio than in Stokes regime because front incoming-flow has to overcome the rear incoming-flow

Stokes and inertial regimes and beyond . . .

- Long-range and many-body character of the hydrodynamic interactions $\rightarrow$ chaotic behavior when the number of particles becomes larger than two
- Multi-body hydrodynamic interactions + coupling between hydrodynamics and the micro-arrangement of the particles $\rightarrow$ collective dynamics
- While the suspension cloud may be modeled as an effective medium of excess mass, the discrete nature of the suspension is a fundamental ingredient in understanding the observed phenomena
- Success of point-particle approach (even though excluded volume effects not accounted for!)
- Different regimes: Stokes, inertia, and far beyond . . .

Falling clouds of particles in vortical flows

Marchetti, Bergougnoux & Guazzelli JFM 2020

Part II

Settling particles

Ubiquitous sedimentation

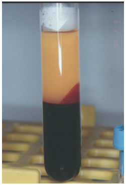


J. Fluid Mech. (1972), *vol.* 52, *part* 2, *pp.* 245–268 245
Printed in Great Britain

Sedimentation in a dilute dispersion of spheres

By G. K. BATCHELOR
Department of Applied Mathematics and Theoretical Physics,
University of Cambridge

(Received 26 August 1971)

The difficulty in the determination of the hydrodynamic interaction of the particles derives from the slowness with which the velocity disturbance in the fluid due to an isolated falling particle decreases to zero at increasing distance and, to a lesser extent, from the random arrangement of the particles in a real dispersion. The magnitude of the fluid velocity at distance r from a single sphere of radius a falling with speed U_0 varies asymptotically as $U_0 a/r$, and so a straightforward attempt to sum the contributions to the velocity at one point from an indefinitely large number of falling spheres in a homogeneous dispersion leads to a series or an integral which diverges strongly. The main objective of work on the problem has been to overcome this obstacle.

There are some common features of the present problem of determining the velocity of sedimentation in a dilute dispersion correct to the order c and the problem of finding one of the bulk transport properties of a dilute dispersion correct to the order c^2, where in both cases c is the volume fraction of the phase present in the form of discrete particles. Included among these transport properties are the effective thermal conductivity of a stationary dispersion, the effective viscosity of a suspension of neutrally buoyant particles in simple shearing motion, and the effective elastic shear modulus for a dispersion of one solid material in another. In all these cases it is necessary to take into account the interaction of different particles, and in all these cases the straight-forward process of summing the separate effects of each of many particles on a given particle is frustrated by failure of the sums to converge absolutely. The general method that has been devised to overcome the difficulties of the present sedimentation problem is expected to be applicable also to these other similar problems.

6. Settling spheres
   - Mean Velocity
   - Velocity fluctuations and hydrodynamic diffusion
   - Microstructure
7. Beyond Stokes: Settling spheres at small inertia
8. Settling fibers
   - The observed regimes
   - Clusters and streamers
   - Structural instability
9. And beyond . . .

Uniformly dispersed spheres

Summing the effects between pairs of particles

- Velocity of a pair of spheres at a separation r:

  $\mathbf{U_S} + \mathbf{\Delta U}$ where $\mathbf{\Delta U}(r)$ incremental velocity due to a second particle

- Averaging over all possible separations which occur with conditional probability $P_{1|1}(r)$

$$\mathbf{U_S} + \int_{r\geq 2a} \underbrace{\mathbf{\Delta U}}_{\frac{a\mathbf{U_S}}{r}} \underbrace{P_{1|1}(r)}_{ng(r)=n} \, dV$$

- Divergence with the size L of the vessel as

$$\int_{2a}^{L} r^{-1} r^2 dr \sim L^2$$

Strong divergence due to long-range hydrodynamic interactions

Sedimentation of spheres in a vessel

Hindered settling

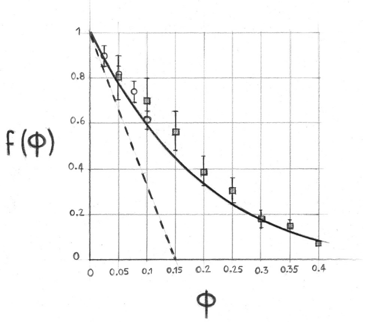

Ham & Homsy IJMF 1988

Nicolai, Herzhaft, Hinch, Oger & Guazzelli PoF 1995

- Mean velocity:

$$\langle \mathbf{u} \rangle_p = \mathbf{U_S} f(\phi)$$

  Richardson-Zaki 1954: $f(\phi) = (1-\phi)^n$ with $n \approx 5$ at low Re
- Main effect = Back-flow
- Renormalization of hydrodynamic interactions: $f(\phi) = 1 + S\phi + O(\phi^2)$ with $S = -6.55$ assuming uniformly dispersed rigid spheres
  Batchelor JFM 1972
- Results depend on **microstructure** in turn determined by hydrodynamics

Velocity fluctuations

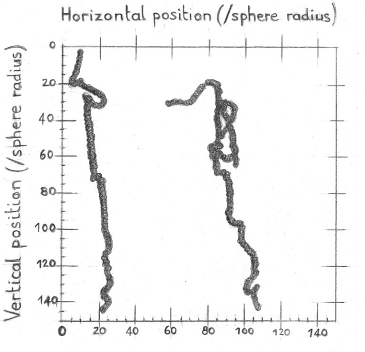

Ham & Homsy IJMF 1988

Nicolai, Herzhaft, Hinch, Oger & Guazzelli PoF 1995

- Random walk through the suspension after a large enough number of hydrodynamic interactions
- Diffusive nature of the long-time fluctuating particle motion
- Anisotropic hydrodynamic self-diffusivities
- Large velocity fluctuations of the same order as the mean particle velocity
- Anisotropic fluctuations with a larger value in the direction of gravity

Divergence paradox for the velocity fluctuations

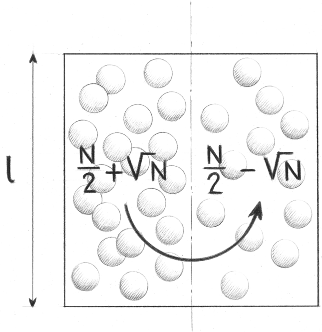

'Blob' of size l ($a\phi^{-1/3} < l < L$) containing $N = \phi l^3/a^3$ spheres

Caflisch & Luke 1985; Tory & Pickard 1986; Hinch 1988

- Random mixing of the suspension creates statistical fluctuations of $O(\sqrt{N})$ on all length-scales l
- Fluctuations in the weight $\sqrt{N}\frac{4}{3}\pi a^3(\rho_p - \rho_f)g$ balanced by Stokes drag on the blob $6\pi\mu l w'$
- Convection currents, also called 'swirls', on all length-scales l

$$w'(l) \sim \frac{\sqrt{N}\frac{4}{3}\pi a^3(\rho_p - \rho_f)g}{6\pi\mu l} \sim U_S\sqrt{\phi\frac{l}{a}}$$

- Fluctuations on the length-scale of the container are dominant

$$w' \sim U_S\sqrt{\phi\frac{L}{a}} \quad \text{diverge with L}$$

More theories . . .

- Koch & Shaqfeh 1991: Debye-like screening
- Tong & Ackerson 1998: turbulent convection analogy
- Levine *et al.* 1998: stochastic model
- da Cunha 1995, Ladd 2002: impenetrable bottom
- Brenner 1999: wall effect
- Luke 2000: stratification $\rightarrow$ fluctuation decay
- Tee *et al.* 2002, Mucha *et al.* 2003-04: diffusive spreading of the front $\rightarrow$ stratification $\rightarrow$ fluctuation decay
- Nguyen & Ladd 2005: polydispersity $\rightarrow$ stratification
- Hinch 1985, Asmolov 2004, Luke 2005: bottom and top $=$ sink of large-scale disturbances

Relaxation of large-scale fluctuations

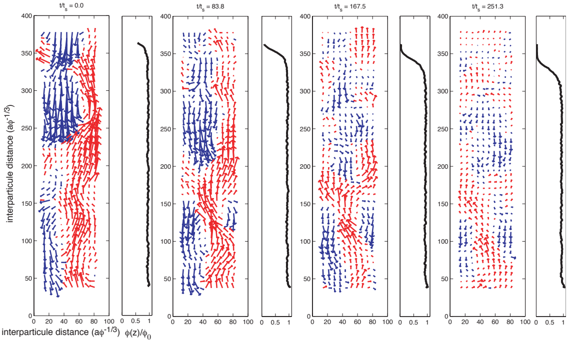

Initially, the large-scale fluctuations dominate the dynamics, in agreement with predicted $w' \sim U_S(\phi \frac{L}{a})^{1/2}$. But, they are transient as the heavy parts settle to the bottom and light parts raise to the top

Guazzelli PoF 2001; Bergougnoux *et al.* PoF 2003; Chehata Gómez *et al.* PoF 2009

Left with smaller-scale fluctuations

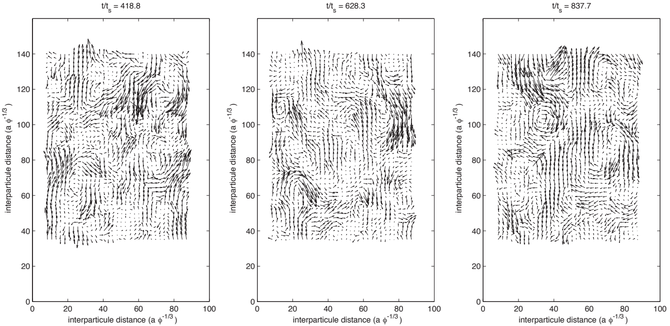

Then, smaller-scale fluctuations (of size $\approx 20\, a\phi^{-1/3}$) are dominant in a steady plateau regime until the arrival of the upper front

Segrè *et al.* 1997; Guazzelli 2001; Bergougnoux *et al.* 2003; Chehata Gòmez *et al.* 2009; Snabre *et al.* 2009

Steady plateau fluctuations

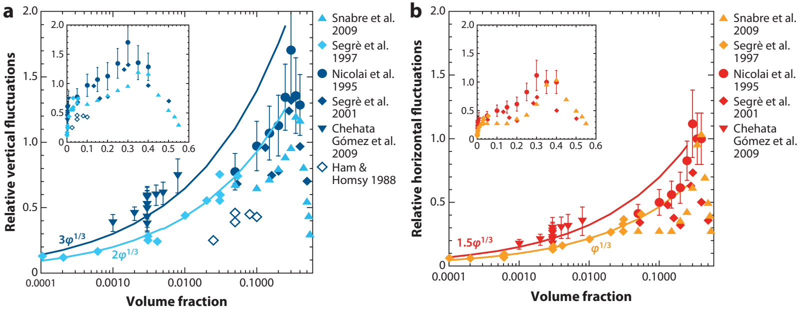

The velocity fluctuations increase roughly as $\phi^{1/3}$ at low ϕ, in agreement with $w' \sim U_S(\phi\frac{\ell}{a})^{1/2}$ with $\ell \approx 20\, a\phi^{-1/3}$. The vertical fluctuations reach a maximum at approximately $\phi = 0.3$, where they are 1.7 times the mean settling speed, and then decrease. The anisotropy between the vertical and horizontal fluctuations is ≈ 2 and even smaller for $\phi > 0.2$.

Particle occupancy distribution in a sheet volume

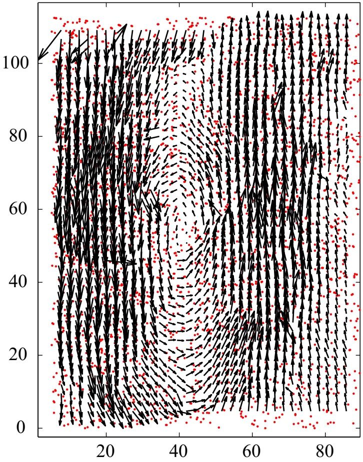

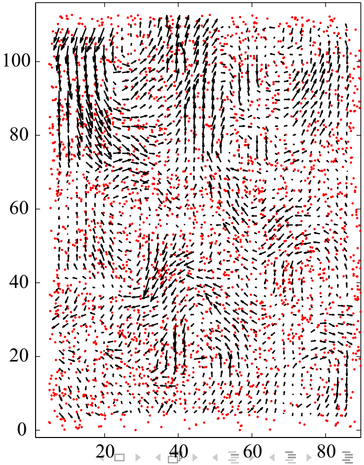

Particle occupancy distribution in a sheet volume

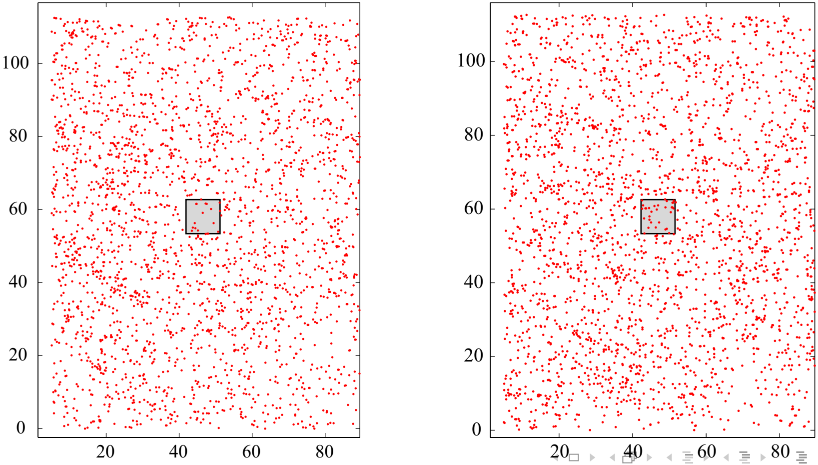

Particle occupancy distribution in a sheet volume

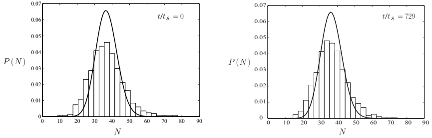

- Similar (rather symmetric) distributions at initial time and in the plateau region
- Slightly shorter and fatter than a Poisson distribution

Slightly sub-homogeneous structure
(in the sense that the variance grows faster than the mean)

Bergougnoux & Guazzelli PoF 2009

σ_N versus $\langle N \rangle$ for different sampling boxes

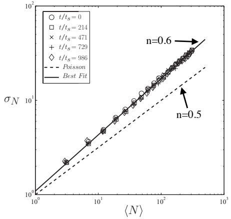

- Not a perfect random positioning of the particles: $\sigma_N = \langle N \rangle^n$ with $n > 0.5$ increasing with increasing polydispersity and ϕ and decreasing with confinement
- No evolution of this power law with time until the sedimentation front enters the imaging window

Screening of the fluctuations by inertia

$Re_a = \rho_f a U_S/\mu \ll 1$ whereas $Re_L = \rho_f L U_S/\mu = Re_a L/a > 1$

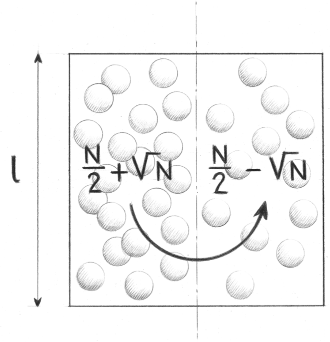

Hinch 1988; Brenner 1999 (alternative argument leading to the same scaling)

- Initial large-scale convection currents limited by inertial forces $\rho_f w'^2 l^2$ rather than by viscous forces $6\pi\mu l w'$

$$w' \sim \sqrt{ag}\,\phi^{1/4}(l/a)^{-1/4}$$

- Large-Re_L prediction shows a decrease with the size of the container whereas the Stokes-regime prediction shows an increase
- Expected fluctuations with length-scale at the crossing

$$w' \sim U_S\,\phi^{1/3} Re_a^{-1/3}$$

Screening of the fluctuations by inertia with a decrease in fluctuations scaling as $Re_a^{-1/3}$

Velocity-field structure for small Re_a but finite Re_L

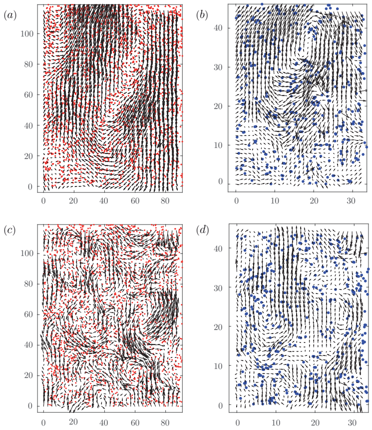

Same relaxation of large-scale fluctuations as observed in the Stokes regime for dilute ($\phi = 0.003$) sedimenting suspensions in large containers (larger than $20\, a\phi^{-1/3}$) when inertia is progressively increased

Bergougnoux & Guazzelli JFM 2021 (special JFM Volume in celebration of the George K. Batchelor centenary)

Plateau velocity fluctuations versus (*a*) Re_a and (*b*) Re_L

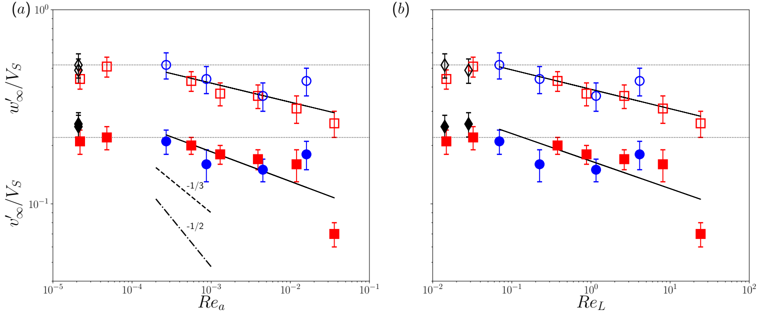

- $Re_a \lesssim 4\,10^{-4}$ or $Re_L \lesssim 0.1$: Stokes regime of constant fluctuations $\frac{w'_\infty}{U_S} \approx 0.52$ and $\frac{v'_\infty}{U_S} \approx 0.22$
- $Re_a \gtrsim 4\,10^{-4}$ or $Re_L \gtrsim 0.1$: Decrease of fluctuations with increasing inertia $\sim Re_a^{-0.1}$ and $\sim Re_L^{-0.1}$

Scaling argument for weak inertia

$Re_a = \rho_f a U_S/\mu \ll 1$ whereas $Re_L = \rho_f L U_S/\mu = Re_a L/a \sim O(1)$

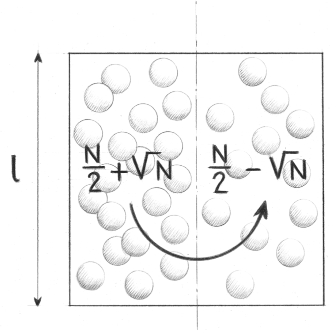

'Blob' of size l ($a\phi^{-1/3} < l < L$) containing $N = \phi l^3/a^3$ spheres

- Statistical fluctuations of $O(\sqrt{N})$, also called 'blob', on length-scale l
- Fluctuations in the weight $\sqrt{N}\frac{4}{3}\pi a^3(\rho_p - \rho_f)g$ balanced by transitional drag on the blob $6\pi\mu l w' \mathcal{F}(Re_l)$ with $Re_l = \rho_f l U_S/\mu = Re_a l/a$
- Convection currents on length-scale l

$$w'(l) \sim \frac{U_S}{\mathcal{F}(Re_l)}\sqrt{\phi\frac{l}{a}}$$

with $\mathcal{F}(Re_l)$ given by correction of
Oseen: $1 + 3Re_l/4$
Schiller-Naumann: $1 + 0.15Re_l^{0.687}$

Plateau velocity fluctuations versus Re_a

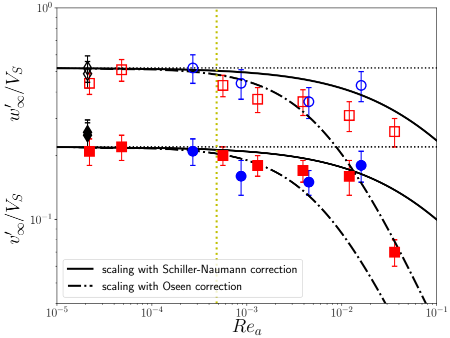

- Decent agreement with Schiller-Naumann correction for a constant ultimate blob size $l \approx \ell_\infty^{||} \approx \ell_\infty^{\perp} \approx 30a\phi^{-1/3}$
- Onset of inertial effect for $Re_l = \rho_f l U_S/\mu = Re_a l/a \sim 0.1$ $\rightarrow \quad Re_a^c \sim 5\,10^{-4}$

Reduction of the fluctuations due to the small inertial increase of the drag on the density fluctuation blob

Bergougnoux & Guazzelli JFM 2021 (special JFM Volume in celebration of the George K. Batchelor centenary)

Particle occupancy distribution in a sheet volume

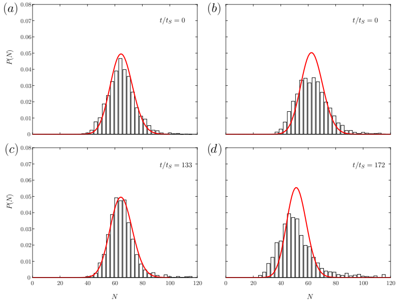

(a),(c) $Re_L = 0.07$ and (b),(d) $Re_L = 4.20$

- Stokes regime: similar (rather symmetric) distributions at initial time and in the plateau region close to Poisson (slightly shorter and wider)
- Weak-inertia regime: distribution at initial time (due to the initial mixing) rather symmetric whereas positively skewed at later times

σ_N versus $\langle N \rangle$ for different sampling boxes

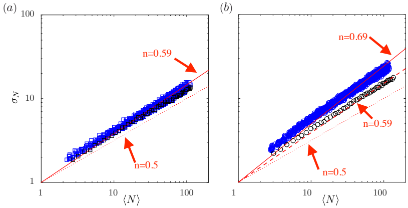

(a) $Re_L = 0.07$ and (b) $Re_L = 4.20$

- Stokes regime: close to Poisson, $\sigma_N \sim \langle N \rangle^{0.59}$
- Weak-inertia regime: at $t = 0$ (initial mixing), $\sigma_N \sim \langle N \rangle^{0.59}$ similar to Stokes case whereas at later time $\sigma_N \sim \langle N \rangle^{0.69}$

With increasing inertia, the structure becomes more sub-homogeneous (in the sense that the variance grows faster than the mean): $\sigma_N \sim \langle N \rangle^n$ with $n > 0.5$, increasing with increasing inertia

Sub-homogeneous holely structure revealed by α-shapes

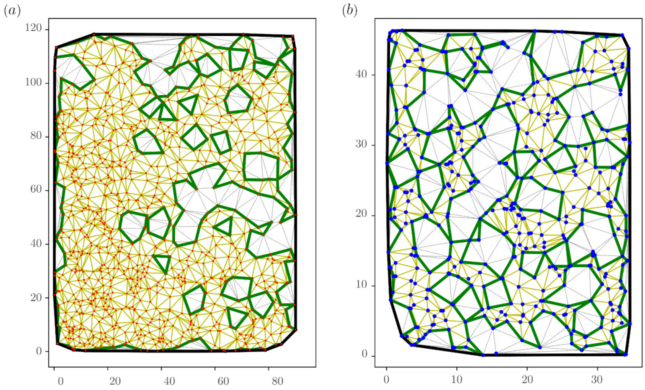

(a) particles of batch A at $Re_L = 24.08$ and (b) particles of batch B at $Re_L = 4.20$ in the plateau region

Large holes having sizes ranging from 5 to a little more than 20 $a\phi^{-1/3}$

6 Settling spheres
- Mean Velocity
- Velocity fluctuations and hydrodynamic diffusion
- Microstructure

7 Beyond Stokes: Settling spheres at small inertia

8 Settling fibers
- The observed regimes
- Clusters and streamers
- Structural instability

9 And beyond . . .

6 Settling spheres
- Mean Velocity
- Velocity fluctuations and hydrodynamic diffusion
- Microstructure

7 Beyond Stokes: Settling spheres at small inertia

8 Settling fibers
- The observed regimes
- Clusters and streamers
- Structural instability

9 And beyond ...

Sedimentation of fibers in a vessel

Mean velocity and orientation in dilute suspensions

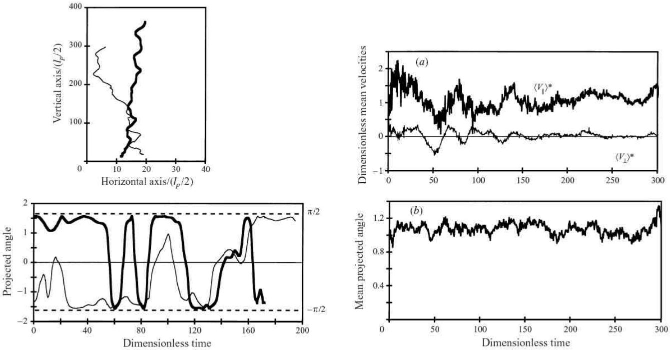

Enhanced sedimentation and vertical orientation

Fiber-tracking in an index-matched suspension ($\phi = 0.005$ and A=11)

Herzhaft, Guazzelli, Mackaplow & Shaqfeh PRL 1996, Herzhaft & Guazzelli JFM 1999

Mean velocity versus concentration

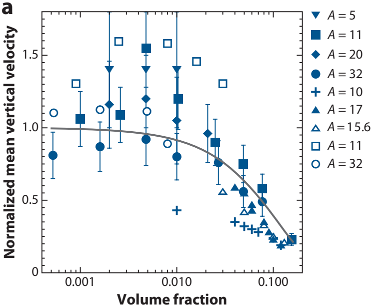

- Experiments: $A = 5$ (filled down-triangles), $A = 11$ (filled squares), $A = 20$ (filled diamonds), $A = 32$ (filled circles) (Herzhaft & Guazzelli 1999), $A = 17$ (filled up-triangles) (Turney *et al.* 1995), $A = 10$ (crosses) (Anselmet 1989)
- Simulations: $A = 15.6$ (open up-triangles) (Mackaplow & Shaqfeh 1998), $A = 11$ (open squares) and $A = 32$ (open circles) (Butler & Shaqfeh 2002)
- Correlation: $(1-\phi)^9$ (solid line)

The mean velocity is found to increase at low ϕ, to reach a maximum (more or less pronounced, depending on aspect ratio, A) at $\phi \approx 0.005$, and then to decrease with increasing ϕ (the hindrance is more severe than in the case of spheres)

6 Settling spheres
- Mean Velocity
- Velocity fluctuations and hydrodynamic diffusion
- Microstructure

7 Beyond Stokes: Settling spheres at small inertia

8 Settling fibers
- The observed regimes
- Clusters and streamers
- Structural instability

9 And beyond . . .

Packet instability → Streamers

Fluorescing fibers within a laser sheet

Metzger, Guazzelli & Butler PRL 2005, Metzger, Butler & Guazzelli JFM 2007

Large-scale streamers

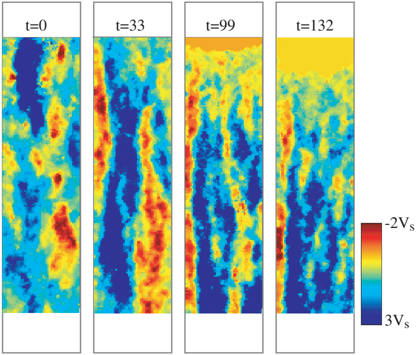

Vertical velocity versus time from PIV measurements

Metzger, Guazzelli & Butler PRL 2005, Metzger, Butler & Guazzelli JFM 2007

Modeling the instability: linear stability analysis

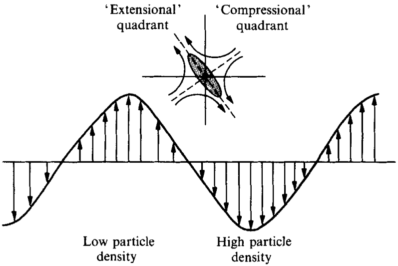

Maximum growth rate for long wavelengths

$\rightarrow$ size of largest possible wavelength $\sim$ container size in bounded systems

BUT not observed experimentally

The instability can be expected to become nonlinear by the time the fibers have fallen through their own length

Koch & Shaqfeh JFM 1989, Guazzelli & Hinch ARFM 2011

Simulating the instability

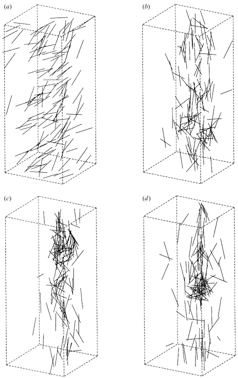

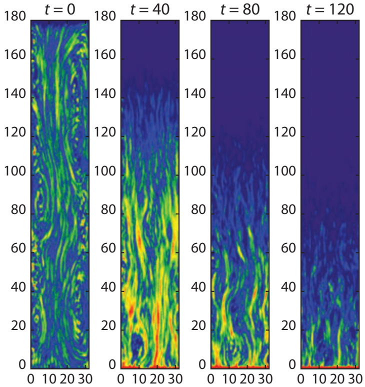

Mackaplow & Shaqfeh JFM 1998, Butler & Shaqfeh JFM 2002, Saintillan, Darve & Shaqfeh JFM 2006, Gustavsson & Tornberg PoF 2009 ...

Simulations versus Experiments

Steady state? Wave-length selection?

Saintillan, Shaqfeh, Darve, Metzger, Guazzelli & Butler APS DFD 2005

Stokes and inertial regimes and beyond ...

- Long-range nature of the multi-body hydrodynamic interactions
  Coupling between hydrodynamics and suspension microstructure
  $\rightarrow$ Collective dynamics: swirls and streamers
- More open problems
  - Larger concentrations
  - Bidisperse or polydisperse particles
  - Anisotropic particles (platelets)
  - Deformable particles: Saintillan *et al.* 2006 ...
  - Non-Newtonian fluids: Mora, Talini & Allain 2005
  - Larger inertia: Koch 1993, Yin & Koch 2007,2008 ...
  - Turbulence: Aliseda *et al.* 2002, Yang & Shy 2005, Bosse, Kleiser & Meiburg 2006 ...